Numerical investigation of detonation combustion wave propagation in pulse detonation combustor with nozzle

Pinku Debnath[*1] and K. M. Pandey[2a]

[1]*Department of Mechanical Engineering, National Institute of Technology Agartala, 799046, Tripura, India*
[2]*Department of Mechanical Engineering, National Institute of Technology, Silchar, Assam,788010 India*

Abstract. The exhaust nozzle serves back pressure of Pulse detonation combustor, so combustion chamber gets sufficient pressure for propulsion. In this context recent researches are focused on influence of nozzle effect on single cycle detonation wave propagation and propulsion performance of PDE. The effects of various nozzles like convergent-divergent nozzle, convergent nozzle, divergent nozzle and without nozzle at exit section of detonation tubes were computationally investigated to seek the desired propulsion performance. Further the effect of divergent nozzle length and half angle on detonation wave structure was analyzed. The simulations have been done using Ansys 14 Fluent platform. The LES turbulence model was used to simulate the combustion wave reacting flows in combustor with standard wall function. From these numerical simulations among four acquaint nozzles the highest thrust augmentation could be attained in divergent nozzle geometry and detonation wave propagation velocity eventually reaches to 1830 m/s, which is near about C-J velocity. Smaller the divergent nozzle half angle has a significant effect on faster detonation wave propagation.

Keywords: detonation wave; nozzle shape; pulse detonation combustor; computational fluid dynamics

1. Introduction

The detonation combustion process generates strong chamber pressure, which requires for achieving high thrust level. Pulse Detonation combustion technology has a great promise for future propulsion application. It has more advantages, which can operate at very high energy densities and it can be developed for simple and compact combustor design. Kailasanath *et al.* (2000, 2005) early reviewed standing normal detonations, pulsed detonation, rotating detonation and oblique shock induced detonation wave. Different design techniques like Schelkin spiral inside the detonation tube and ejector technique can enhance the performance of PDE (Pandey and Debnath 2016, 2017). Mouronval *et al.* (2002) numerically investigated the shock wave starting process of two-dimensional and axsymmetric nozzle flows. They have introduced the faster starting process of shock wave. The nozzle controls the detonation chamber pressure and converts the hot chamber flow into thrust. The contraction ratio of nozzle is designed to maintain pre-detonation chamber pressure (Dyer *et al.* 2003). Chen *et al.* (2012) experimentally investigated the nozzle effects on

---

∗Corresponding author, Assistant Professor, E-mail: er.pinkunits@yahoo.com
[a]Professor, E-mail: kmpandey2001@yahoo.com

thrust and inlet pressure of an air-breathing pulse detonation engine. Their results showed that thrust augmentation of converging-diverging nozzle, diverging nozzle or straight nozzle is better than that of converging nozzle on whole operating conditions. Li *et al.* (2007) conducted an experiment on PDRE model utilizing kerosene as the fuel, oxygen as oxidizer and nitrogen as purge gas. The thrust and specific impulse were investigated in this analysis. Their obtained results showed that the thrust generations of PDRE test model were approximately proportional to combustion wave frequency and time average thrust was observed around 107 N. Yan *et al.* (2011) studied the performance of pulse detonation engine with bell-shaped convergent-divergent nozzle. Their experimental tested result has shown that the maximum thrust augmentation is approximately 21%. Again Yan *et al.* (2011) experimentally investigated injectors and nozzle effect on pulse detonation rocket engine performance. They observed that nozzles are the critical component for improving the performance of PDE. From their tested results they observed that a nozzle with high contraction ratio and high expansion ratio generated the highest thrust augmentation of 27.3%. Allgood *et al.* (2006) experimentally measured the damped thrust of multi cycle pulse detonation engine with exhaust nozzle. Their results showed that diverging nozzle increases the performance with increase in fill-fraction. Further four diverging nozzle and six converging-diverging nozzle were tested experimentally by Cooper *et al.* (2008). Morris *et al.* (2005) conducted numerical simulation for investigating the performance of pulse detonation engine. In this analysis four different types of nozzle geometry are used. Their results indicate that convergent divergent nozzle is greatly more effective than other types of nozzle. Nozzle configurations are often considered as a method to enhance the performance that can be attained from a detonation tube configuration. Therefore, there have been many research efforts about effects of nozzle on the performance of pulse detonation engines (Sutton and Oscar 2010). Later on performance of PDE in subsonic and supersonic flight conditions has been studied by Tangirala *et al.* (2007). Their studies were employed in 2D CFD model. The results showed that exit nozzle enhances thrust generation, maintains operating pressure and also controls operating frequency. The effect of different types of nozzle on continuous detonation engine (CDE) using one step 3-D numerical chemical reaction model has been studied by Shao *et al.* (2010). The four types of nozzle are namely constant-area nozzle, Laval nozzle, diverging nozzle and converging nozzle were studied in this analysis. The results indicated that Laval nozzle has great scope to improve the propulsion performance. Ma *et al.* (2005) studied the comparison between single-tube and multi-tube PDEs and influence on nozzle flow field to improve propulsive performance. They showed that convergent nozzle helps to keep original chamber pressure constant and consequently improves the engine performance. Again Ma *et al.* (2005) presented the thrust chamber dynamics of single and multi-tube design of PDEs. Their results indicated that multi-tube design improved the performance by reducing the degree of unsteadiness in the flow. Specific impulses were obtained 3800s at a flight Mach number of 2.1 with a single converging-diverging exit nozzle. Deflagration to Detonation transmission in abrupt area change is experimentally studied by Hsu *et al.* (2018) between propane/oxygen and propane/air mixture. Kuzmin (2019) studied abrupt changes of shock wave positions under gradual variation of Mach number.

It has been realized that numerical and experimental researches on nozzle effect on in pulse detonation combustion have been reported in the past few years that nozzles are also helpful for improving the PDE performance. However, which kind of nozzle is appropriate for performance enhancement is still in debate. In this research paper different type of nozzle like convergent-divergent nozzle, convergent nozzle, divergent nozzles are used at exit section of detonation tube to simulate the detonation wave structure.

Table 1 The series of nozzle dimensions at exit section of PDE

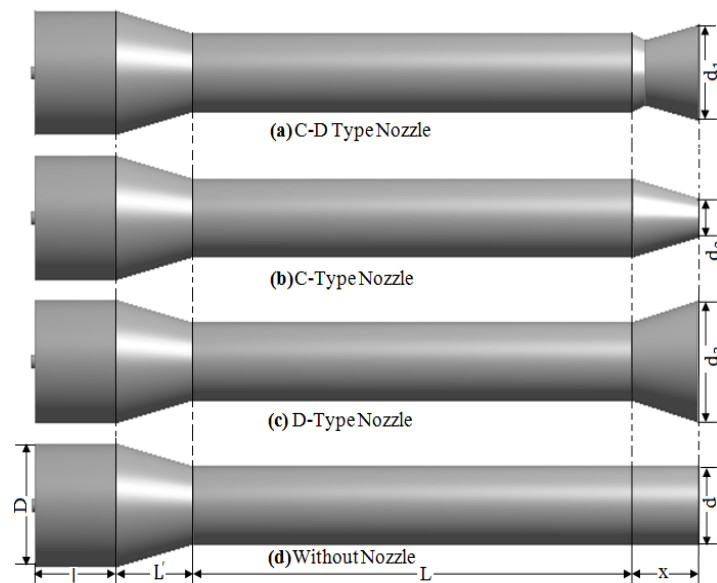| Nozzle Type/ Dimension(cm)	Convergent Divergent Nozzle	Convergent Nozzle	Divergent Nozzle	Without Nozzle
Length (x)	9	9	9	9
Inlet Diameter (d)	6	6	6	6
Exit Diameter (d_1, d_2, d_3, d)	7.3	3	9.3	6
Throat Diameter	5	-	-	-
Exit Nozzle Area (cm^2)	41.85	7.07	67.93	28.27

Fig. 1 Physical model of PDE with (a) convergent divergent nozzle, (b) convergent nozzle, (c) divergent nozzle and (d) clean configuration at exit section of detonation tube

2. Physical model of PDE with nozzle series

The physical models of PDE with different nozzle geometry are shown in Fig. 1. Table 1 represents the dimension of nozzle series. The nozzles are used at the exit of detonation tube. The detonation tube having length of L=60 cm and 6 cm diameter (d). The diameter (D) of combustion chamber is 9.5 cm and length of l=11 cm. The distance between combustion chamber and detonation tube having length of L'=10.5 cm.

3. Geometry model of half angle and length of nozzle

The divergent angle of nozzle selection segment has a low divergence loss as the combustion product leaves the nozzle exit plane. Table 2 represents the series of divergent nozzle dimension at exit of PDE with different half angle and nozzle length. The PDE combustion chamber length, diameter and detonation tube length, diameter dimension are same as earlier one from Table 1.

Table 2 The series of divergent-nozzle dimensions at exit section of detonation tube

Length (cm)/ Exit Diameter (cm)	8° Half angle	12° Half angle	15° Half angle
7	7.968	8.98	9.75
8	8.248	9.40	10.28
9	8.52	9.83	10.82
10	8.81	10.25	11.35

4. Computational methodology

4.1 Mesh generation of computational domain

Fig. 2 shows the computational domain with tetrahedral mesh. Tetrahedral mesh was taken for discretized the computational domain. The inlet boundary conditions are applied to the fuel and air at inlet (flow) conditions also represented in this Fig. 2.
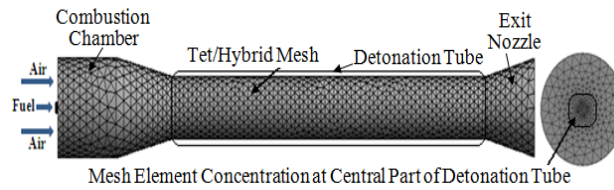

Fig. 2 Tet/Hybrid mesh generation and boundary details of computational domain

Table 3 Numbers of nodes and elements corresponding to mesh size

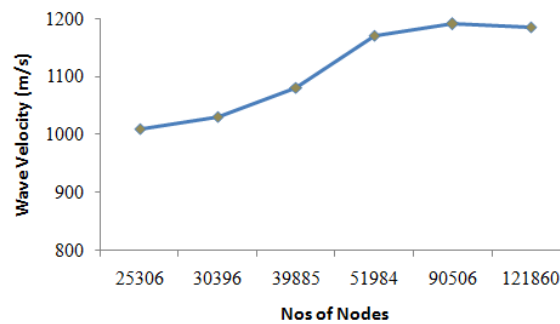| Refinement level	Number of Nodes	Number of Elements
1	25306	128061
2	30396	153500
3	39885	203994
4	51984	266336
5	**90506**	**484504**
6	121860	651624

Fig. 3 Grid independence study of PDE with divergent nozzle

4.2 Grid independence study

The computational mesh generation of pulse detonation engine with D-type nozzle has been shown in Fig. 3. It includes the combustion chamber, detonation tube and divergent nozzle at exit section of detonation tube. The PDE with convergent, convergent-divergent and without nozzle are also discretized into small unstructured triangular cells for simulation. The accuracy of post processor CFD solution is governed by the number of cells in the mesh within the computational domain. The Table 3 represents the number of nodes and elements corresponding to mesh size of divergent PDE configurations. After a particular refining limit, the post processor results changes no more. At this point, it is said that grid independence in meshing is achieved. The PDE with divergent nozzle has shown grid independence test and it has been verified and shown in Fig. 3. The number of elements of other nozzle configuration are varies in between 411984 to 621860.

4.3 Boundary conditions for simulation

The boundary condition of computational domain has been shown in Fig. 2. The incoming air-fuel flow rate to the combustor conditions are coaxial supersonic flow at Mach number of 1.4. The initial combustion temperature of 298 K and hydrogen mass flow rate of 0.089 kg/s with air fuel ratio of 14.91:1 has been taken for simulation initialization. The outer surface of combustion chamber, detonation tube and nozzle are considered as adiabatic walls. The exit nozzle areas are considered as a pressure outlet. The propagation of fuel air mixture takes place inside the combustor through auto-ignition.

4.4 Framework of governing equation

The details formulation is based on the conservation equations of mass, momentum, energy and species concentration. To determine the flow dynamics and propulsive performance of PDE the diffusive effects are neglected. A one step chemical reaction model is used in this simulation. The resultant three dimensions Euler equations in generalized coordinates are used as governing equations and can be written in the following vector form:

$$\frac{\partial U}{\partial t}+\frac{\partial E}{\partial \xi} + \frac{\partial F}{\partial \eta} + \frac{\partial G}{\partial \zeta} = S \tag{1}$$

where the dependent variable vector U, convective flux vectors E, F and G and source vectors S are defined as

$$U= [\rho \quad \rho u \quad \rho v \quad \rho w \quad e \quad \rho \beta]^{T}$$

$$S= [0 \quad 0 \quad 0 \quad 0 \quad 0 \quad \rho \dot{\omega}_{\beta}]^{T}$$

$$E = [\rho \bar{U} \quad \rho \bar{U} u +p\xi_{x} \quad \rho \bar{U} v +p\xi_{y} \quad \rho \bar{U} w +p\xi_{z} \quad \bar{U}(p+e) \quad \rho \bar{U} \beta]^{T}$$

$$F= [\rho \bar{V} \quad \rho \bar{V} u +p\eta_{x} \quad \rho \bar{V} v +p\eta_{y} \quad \rho \bar{V} w +p\eta_{z} \quad \bar{V}(p+e) \quad \rho \bar{V} \beta]^{T}$$

$$G = [\rho \bar{W} \quad \rho \bar{W} u +p\zeta_{x} \quad \rho \bar{W} v +p\zeta_{y} \quad \rho \bar{W} w +p\zeta_{z} \quad \bar{W}(p+e) \quad \rho \bar{W} \beta]^{T}$$

$$\bar{U}=u\xi_{x} + v\xi_{y} + w \ \xi_{z}$$

$$\bar{V}= u\eta_{x} + v\eta_{y} + w \ \eta_{z}$$

$$\bar{W}= u\zeta_{x} + v\zeta_{y} + w \ \zeta_{z}$$

The pressure p and total energy e are calculated using equations of state

$$P = \rho RT$$

$$E = \frac{p}{\gamma - 1} + \beta \rho q + \frac{1}{2}\rho u^2 + \frac{1}{2}\rho v^2 + \frac{1}{2}\rho w^2$$

where ρ is density, R gas constant, T temperature, γ specific heat ratio and q heat release per unit mass. The mass production rate is

$$\dot{\omega} = \frac{d\beta}{dt} = -AB \exp(-E_a/(RT)) \tag{2}$$

where β is the mass proportion of reaction mixture gas ($\beta = 1$ represents a fresh gas mixture, whereas $\beta = 0$ indicates the detonation products are in equilibrium). It is ensured that the thermodynamics parameters are optimized to predict the C-J detonation wave speed within the range of initial boundary conditions.

5. Validation of present work

The combustion chamber is defined as deflagration combustion zone and detonation tube is defined as detonation combustion zone. The computational simulations are fully agreed with experimental results, which have been cited from literature. The present investigated detonation wave speed is 1830 m/s, which is observed from velocity contour plot analysis and it is comparatively higher than the detonation wave speed of 1666.67 m/s, 1538.46 m/s and 1694.9 m/s at different location in detonation tube respectively (Chen *et al.* 2012). Rapid propagation of detonation wave and fully developed Chapman Jouguet detonation wave is essential to enhance propulsive thrust.

6. Results and discussions

6.1 Contour plot analysis

Fig. 4 shows the contour of static temperature for aforesaid nozzles at single time step simulation. The propagation temperature of deflagration combustion wave was observed in PDE with clean configuration of detonation tube. This strong propagation temperature definitely increases the thermodynamics performance of PDE. Pulse detonation combustor having a clean configuration is quite different from aforesaid nozzles. The combustion wave propagation temperature magnitude of 3210 K is constant at combustor and gradually decreases at end of detonation tube.

The fuel and oxidizer are injected with low pressure in combustion chamber, after combustion it accelerates and produced strong thrust. The detonation combustion wave pressure has great influence for propulsive performance enhance the PDE. The combustion wave flow field structure during the cycle operations are obtained by dynamic pressure contour analysis. Fig. 5 illustrates the successive contour plots of dynamic pressure for aforesaid four different types of nozzle. The successive combustion wave pressure was observed at detonation tube exit section. A nozzle with large expansion area causes lower pressure and strong velocity wave in detonation tube. The exhaust combustion wave pressures are responsible for thrust calculation. From C-D type nozzle
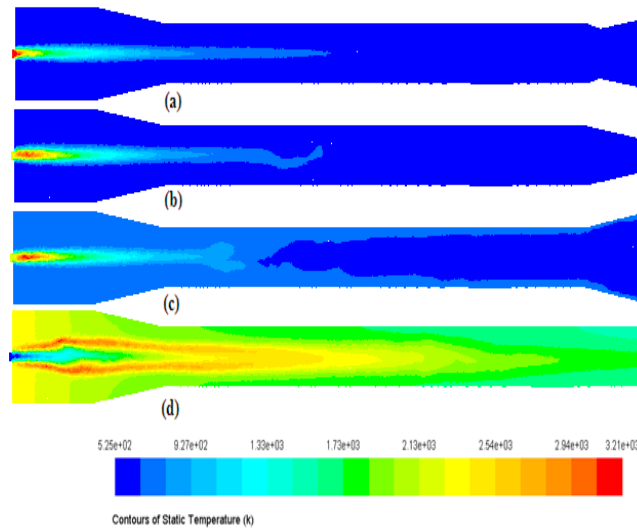
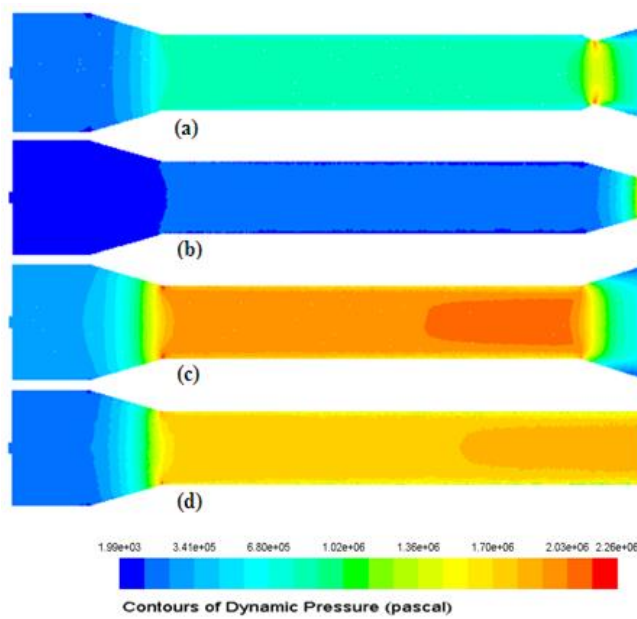Fig. 4 Contour of static temperature of combustion wave

Fig. 5 Detonation wave dynamic pressure (Pascal) contours for (a) convergent divergent nozzle, (b) convergent nozzle, (c) divergent nozzle and (d) clean configuration

average dynamic pressure of 17.9×10^5 Pascal was obtained, for C type nozzle maximum exit dynamic pressure of 107×10^5 Pascal was obtained from blow down operations. Using D type nozzle maximum exit dynamic pressure was obtained 7.65×10^5 Pascal. From without nozzle configuration average dynamic pressure of 7.53×10^5 Pascal was obtained. The variation of pressure magnitude of 20.8×10^5 Pascal was found in C-D type nozzle. From C type nozzle

maximum exit dynamic pressure was obtained 126×10^5 Pascal. From D type nozzle average dynamic pressure was obtained 9×10^5 Pascal. From without nozzle maximum exit dynamic pressure was obtained 8.88×10^5 Pascal as shown in Fig. 5. The detonation wave dynamic pressure characteristics in detonation tube during the flame propagation and deflagration to detonation transition is obtained from contour plots analyses. The weak detonation wave propagates to combustor in subsonic condition with low Mach number and the flow is almost isobaric. The strong detonation wave pressure associated with exhaust flow from detonation tube and nozzle preserves the chamber pressure during the blow down. Although C-D type nozzle configuration peak dynamic pressure of 18.1×10^5 Pascal in throat section, but pressure is weak in detonation tube. Fig. 5(b) shows the average dynamic pressure of 0.892×10^5 Pascal was found in detonation tube with C-type nozzle. In this configuration combustion wave is decelerates due to convergent nozzle. In D-type nozzle strong wave was developed in detonation tube with a magnitude of 10.3×10^5 Pascal dynamic pressure and 3.11×10^5 Pascal was found in combustion chamber. In large scale pressure difference ($P_e > P_\infty$) flame propagates at high flow momentum jetting, jet-like flow enhances flame acceleration and flame pressure seems to rise gradually until it is equal to optimum Chapman-Jouguet values. Fig. 5(d) shows the dynamic pressure tail off augmentation with magnitude of 8.83×10^5 Pascal in detonation tube. The contours plots clearly show that detonation waves are strong in D-type nozzle configuration and it enhances the pressure thrust.

The detonation tube is a responsible for leading detonation wave structure. The overall combustion wave velocity rises in detonation tube, which enhances the propulsion performance. The detonation wave pressure is weak in combustion chamber due to convergent nozzle at exit section. Fig. 6 illustrates the successive velocity contour plot of detonation wave at different locations at various Mach numbers for four nozzle geometry conditions. Each nozzle exit velocity is required for thrust calculation. In C-D type nozzle average exit velocity magnitude was obtained 1630 m/s as shown in Fig. 6. Using C type nozzle average exit velocity magnitude was obtained 1180 m/s. Using D type nozzle the velocity magnitude was obtained 1100 m/s at Mach number of 1.2. Without nozzle average velocity was obtained as same as D type nozzle. The velocity variations are obtained for above mention nozzles are 1760 m/s for C-D type nozzle. Using C type nozzle average exit velocity magnitude was obtained 1530 m/s. Using D type nozzle velocity of 1190 m/s was obtained and without nozzle configuration average velocity was obtained same as D type nozzle at Mach number of 1.4. Fig. 6 illustrates the successive detonation wave contours at four analyzed nozzle configurations at optimum Mach number of 1.4. The turbulence flame front of detonation wave was developed usually at high velocity (supersonic condition) and it depends on exit nozzle. In supersonic flow condition Mach number of detonation wave is high, so there is no vortex in detonation tube. The Chapman Jouguet (C-J) velocity of detonation wave dominates the identical velocity for strong detonation wave. The detonation wave speed depends on shape of exit nozzle. From the contour plot analysis clearly shows that in C-D type nozzle average detonation wave travels with velocity magnitude of 827 ± 100 m/s. The detonation wave propagates at speed of 995 ± 50 m/s at C-type nozzle configuration as shown in Fig. 6(b), then detonation wave gradually decays to the C-J detonation speed and wave speed goes at subsonic (Ma<1) conditions in combustion chamber. In D-type nozzle configuration flow is expanded to become supersonic and finally the wave velocity reaches the C-J velocity with magnitude of 1180 ± 100 m/s. The large velocity gradient contour field enhances the flame stretching, in this situation Mach stem is generated in detonation tube. Figs. 6(c) and 6(d) have shown that there is no remarkable
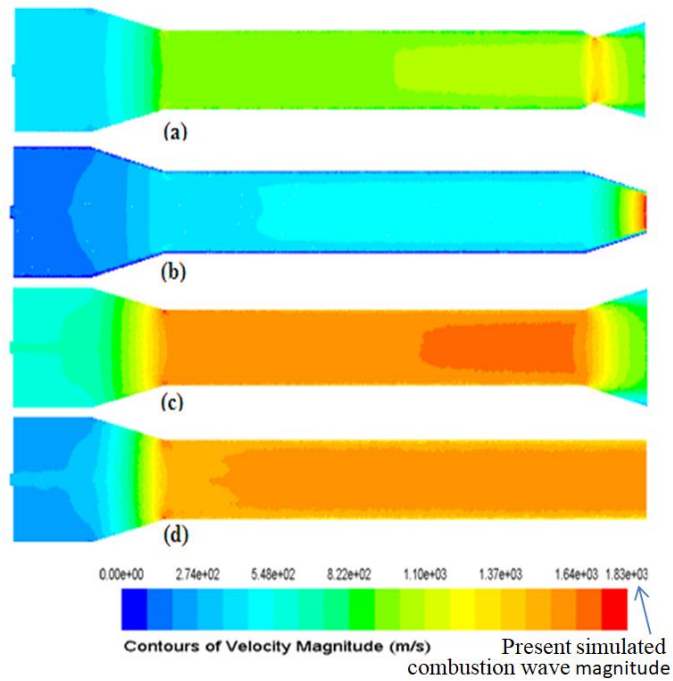
Fig. 6 Detonation wave velocity (m/s) magnitude contours for (a) convergent divergent nozzle, (b) convergent nozzle, (c) divergent nozzle and (d) clean configuration
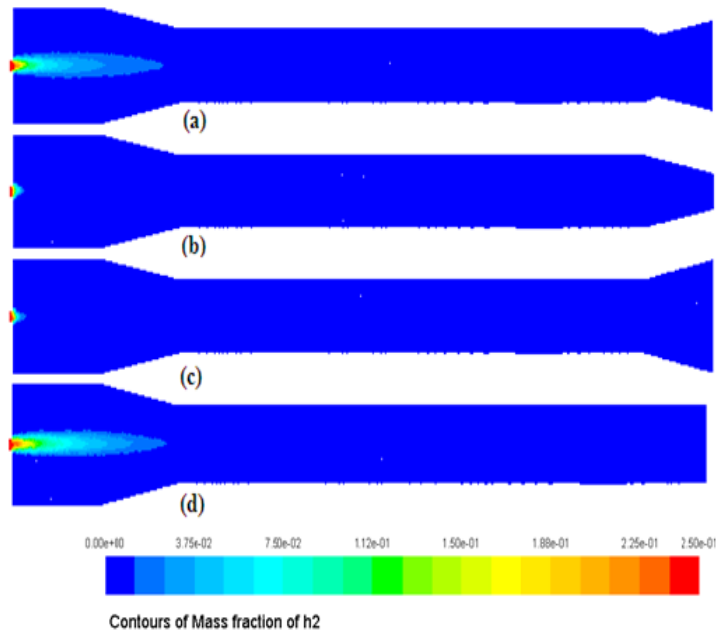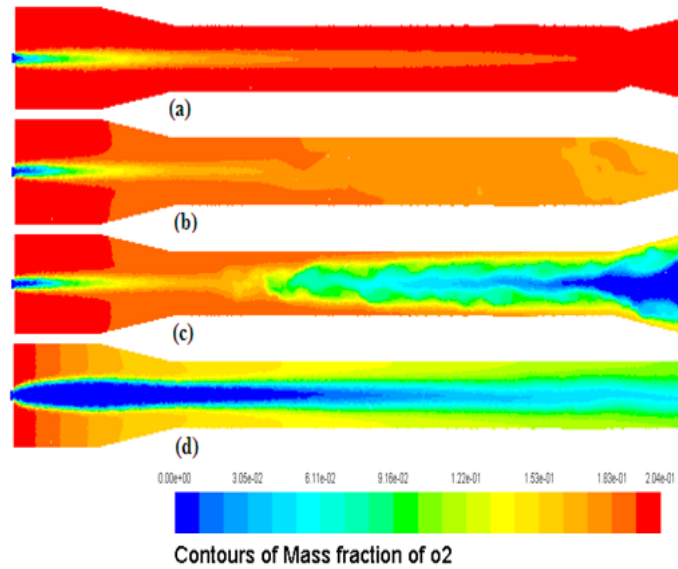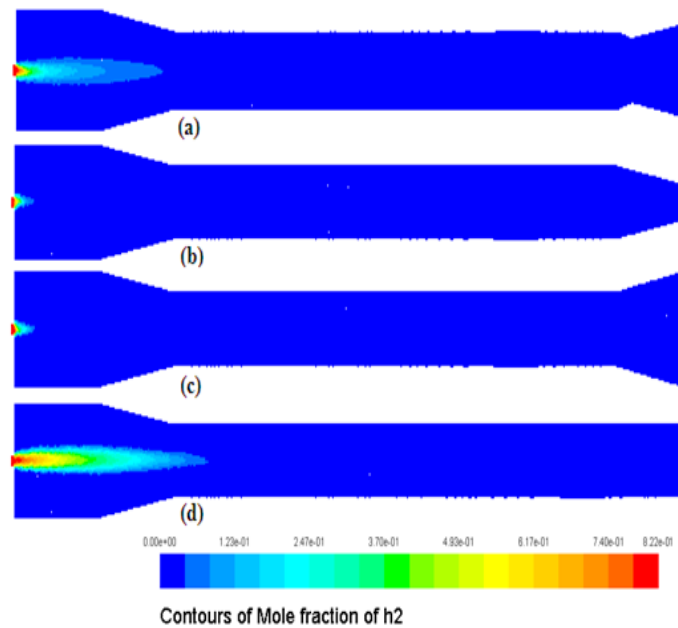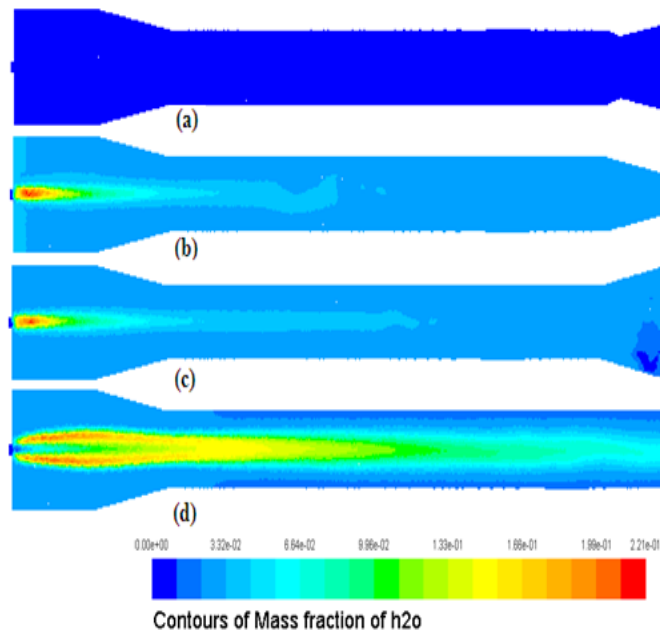

Fig. 7 Contour of H_2 mass fraction

difference in detonation wave speed between the D-type nozzle and clean configuration. The

Fig. 8 Contour of O_2 mass fraction of combustion product

Fig. 9 Contour of mole fraction of H_2

contour plot clearly indicates that detonation wave speed successfully reaches to 1830 m/s which are near about C-J velocity at D-type nozzle and clean configuration.

Fig. 7 shows the H_2 mass fraction contour at four aquatint nozzles. Among the four type of nozzle the strong H_2 mass fraction was observed at PDE combustor with clean configuration. Fig. 8 shows the O_2 mass fraction contour plots in four aforesaid nozzles. Simulated O_2 mass

Fig. 10 Contour of mass fraction of H_2O

fraction was observed at straight nozzle configuration compared with other nozzle geometry. Unburned combustion product was observed at divergent and convergent nozzle configuration. The O_2 mass fraction varies for minimum 0.0305 to 0.20, which as shown in contour plot analysis. The complete fuel-air burning flame of hydrogen mole fraction was observed at clean configuration as shown in Fig. 9(d). The density of hydrogen mole fraction was found in PDE combustor with clean configuration. Fig. 10 shows the analogous contour plots histories of H_2O in four cases of nozzle geometry. The reacting mass fraction of water vapor varies from 0.332 to 0.221. Wider water vapor mass fraction was observed in straight detonation tube which as shown in Fig. 10(d). The concentration of water vapor mass fraction gradually decreases at end of detonation tube. Stronger detonation wave always accelerate in lesser water vapor concentration zone.

6.2 Performance analysis

6.2.1 Pressure distribution along the combustor

The pressure distributions along the PDE combustor are shown in Fig. 11. The maximum effective pressure was found at 0.515 wave travelling distance in PDE combustor. It also observed that mean effective pressure magnitude of 12.5 MPa in detonation tube with divergent nozzle.

6.2.2 Propulsion thrust analysis

The propulsion thrust is calculated in PDE with aforesaid nozzle by assuming an isentropic expansion of the combustible product to normal atmospheric condition.

$$F = \dot{m}_{exit} \sqrt{2c_p T_t \left[1 - \left(\frac{P_a}{P_t}\right)^{\frac{\gamma-1}{\gamma}}\right]} \tag{3}$$
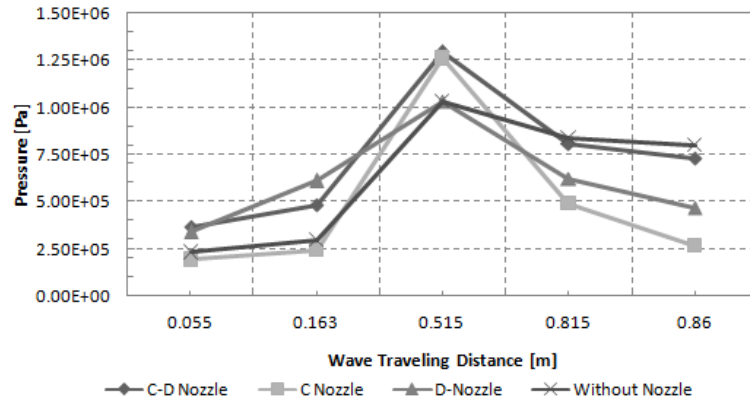
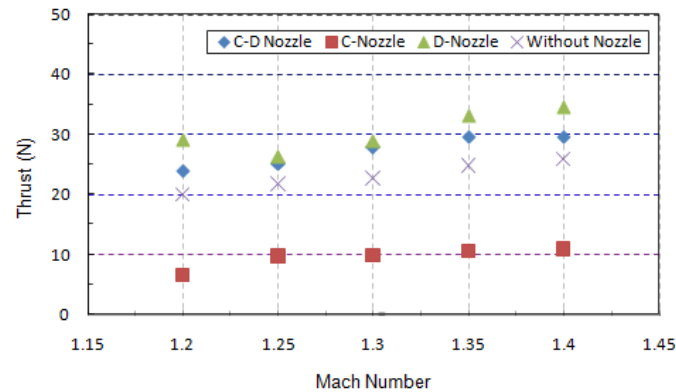Fig. 11 Pressure distribution along the PDE combustor

Fig. 12 The thrust variation for C-D nozzle, C-nozzle, D-nozzle and without nozzle configuration at different Mach number

where subscript "a" indicates the ambient state which sets the nozzle discharge static pressure. Subscript "t" stands for stagnation condition.

The net thrust is calculated based on respective nozzle configuration. Fig. 12 shows the variation of thrust with Mach number for aforesaid nozzle and Mach numbers depend on incoming flow rate of combustible mixture in combustor. The net thrust gradually increases with increasing Mach number for aforesaid nozzle configuration and propulsion thrust improves with increase in nozzle exit section area. Although the net thrust of C-D type and without nozzle are almost equal, but in whole operating conditions D-type nozzle thrust is more efficient. The net thrust of 29.95 N, 34.49 N and 25.89 N were obtained from C-D type, D-type and without nozzles at optimum Mach number of 1.4. The maximum thrust 34.49 N was obtained from divergent nozzle configuration. Fig. 12 also represents that thrust augmentation of D-type nozzle with magnitude of 26.07 N, 26.36 N, 28.95 N, 33.16 N and 34.49 N are the best compared to other type of nozzle at aforesaid Mach numbers. The thrust generation increases with increasing the operating Mach number in supersonic conditions.

6.2.3 Effect of nozzle half angle and length
The combustion wave velocity fluctuates eventually by changing the initial boundary
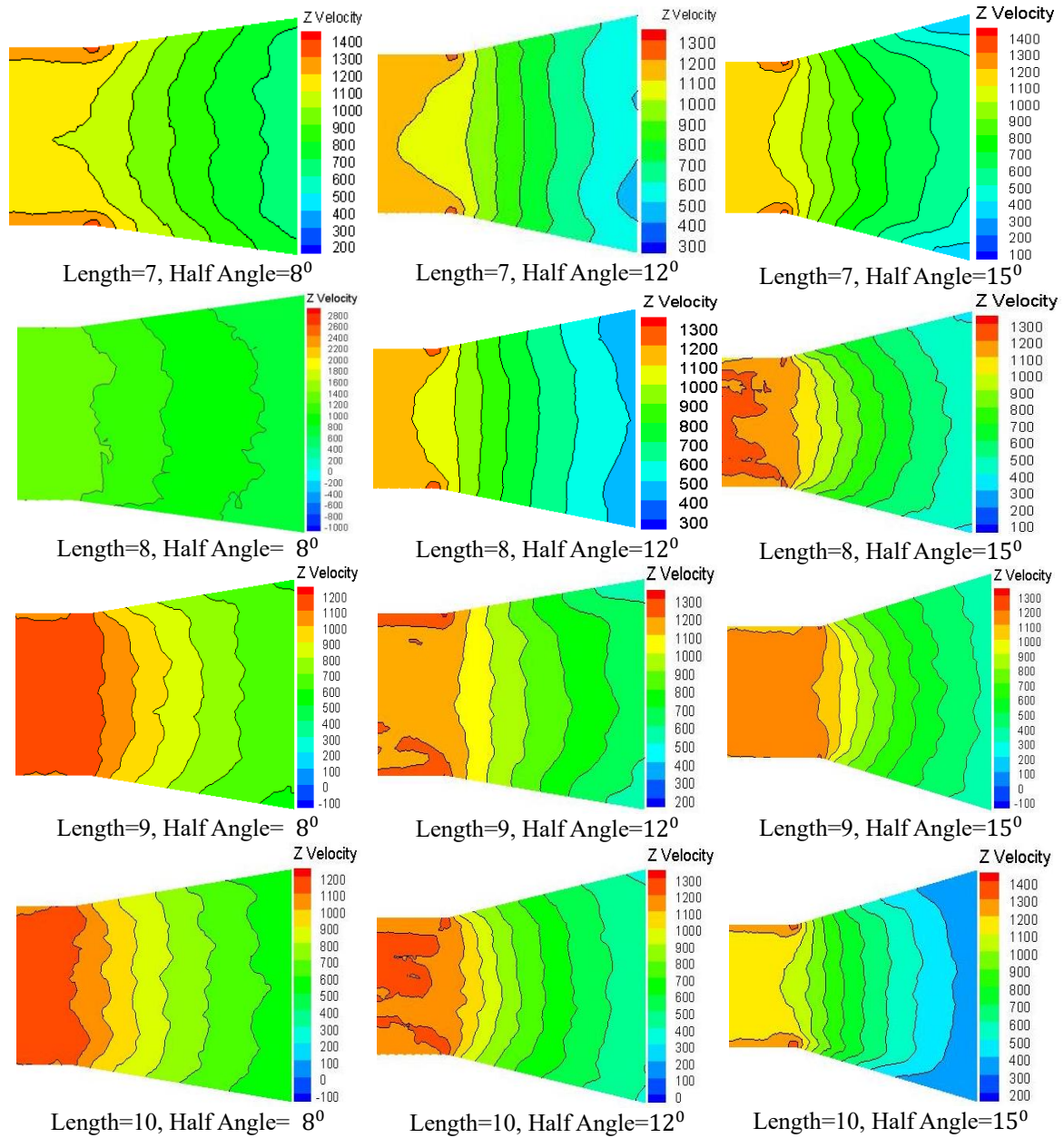
Fig. 13 Comparison of instantaneous detonation wave velocity flow field structure contour based on different half angle and nozzle length at a glance

conditions. After complete combustion blow down process is an important that enhances the thrust which is generated by PDE cycle. The steady combustion wave flow field contour have shown in twelve divergent nozzle geometry in exit section of pulse detonation combustor at a glance as shown in Fig. 13. The compressibility effects of combustion wave are presented in exit nozzle section due to nozzle half angle varies. For the reason of nozzle configuration change, the

detonation wave goes a first compression and later on expansion due to nozzle shape changes. The accelerating process of detonation wave depends on divergent angle changes. The detonation combustion wave flows through the divergent section and it is changed in front of throat section. The speed of detonation wave was calculated from post processing CFD simulation. The detonation wave propagation velocities of 1400 m/s are obtained at Mach number of 1.4. The optimum momentum thrust depends on selection of divergent nozzle geometry and it was described by velocity flow field structure. The strong momentum thrust can be achieved from wave velocity and it depends on optimum nozzle geometry and half angle. The combustion wave velocity produces more thrust, as thrust increases combustion product velocity increases. The nozzle lengths are 7, 8, 9 and 10 in cm and half angles of $8°$, $12°$ and $15°$ are analyzed by velocity contour flow field structure. From literature survey the maximum length is restricted by PDE geometry. The contour plots show that variable nozzle geometry is needed to produce an appropriate level of detonation wave velocity. The largest divergent half angles continuously delay the detonation wave propagation. The divergent nozzle achieves the strongest expansion detonation wave. The small nozzle length and small half angle are having more effect on the velocity. The velocity decreases more rapidly in the exit section of detonation tube. The contour plots show that detonation wave velocity are varying in between 1200 m/s to 1400 m/s at nozzle length of 9 cm and $8°$ half angle, nozzle length of 10 cm and $8°$ half angle, nozzle length of 9 cm and $12°$ half angle, nozzle length of 8 cm and $15°$ half angle. Lesser the nozzle half angle faster the detonation wave starting process.

7. Conclusions

The detonation wave propagation temperature, dynamic pressure, wave velocity, mass fraction of combustion products and thrust are affected by nozzle geometry and operating Mach number and also effected by divergent nozzle half angle and length. Further research can be carried out by using unsteady simulation by different time steps. The following conclusions are drawn on the basis of present numerical simulation.

• Higher the operating Mach numbers faster the starting process. From the performance matrices it was concluded that net thrust of 26.07 N, 26.36 N, 28.95 N, 33.16 N and 34.49 N are obtained by rapid change of operating Mach number in between 1.2 to 1.4 in divergent nozzle configuration. These net thrusts are comparatively higher than other aforesaid nozzles. At optimum Ma=1.4, the maximum 34.49 N thrust was obtained. It can be concluded that thrust generation is better in divergent nozzle than convergent-divergent nozzle, convergent nozzle and without nozzle. Another key finding was found that the thrust proportionally increases with Mach number increase in supersonic condition.

• From combustion wave dynamic pressure contour analysis, the strong dynamic pressure wave was found in divergent nozzle at exit section of detonation tube. Although detonation pressure is stronger in case of clean configuration, but magnitude is poor. The strong dynamic pressure magnitude of D-type nozzle is $10.3×10^5$ Pascal, which is higher than other type of nozzles. Taking dynamic pressure point of view PDE with divergent nozzle achieve better thrust augmentation.

• The combustion wave velocity contour plot clearly shows that strong detonation wave initiates in detonation tube with divergent nozzle. The detonation wave accelerates with magnitude of 1830 m/s in divergent nozzle geometry. Such detonation wave speed has not that much

difference from Chapman-Jouguet detonation wave speed. So D-type nozzle is more effective for detonation wave acceleration and propagation in supersonic condition.

• Detonation wave starting is delayed if nozzle angle is increased. The divergent half angle is more effective to accelerate the detonation wave rapidly. So combustion wave reaction contour physics clearly shows those detonation waves are strongly propagating at $8°$ half angle with nozzle length of 9 cm and 10 cm.

References

Allgood, D., Gutmark, E., Hoke, J., Bradley, R. and Schauer, F. (2006), "Performance measurements of multicycle pulse-detonation-engine exhaust nozzles", *J. Propulsion Power*, **22**(1), 70-77. https://doi.org/10.2514/1.11499.

Barbour, E.A., Hanson, R.K., Morris, C.I. and Radulescu, M.I. (2005), "A pulsed detonation tube with a converging-diverging nozzle operating at different pressure ratios", *Proceedings of the 43rd AIAA Aerospace Sciences Meeting and Exhibit*, Reno, Nevada, U.S.A., January.

Chen, W., Fan, W., Zhang, Q., Peng, C., Yuan, C. and Yan, C. (2012), "Experimental investigation of nozzle effects on thrust and inlet pressure of an air-breathing pulse detonation engine", *Chin. J. Aeronaut.*, **25**(3), 381-387. https://doi.org/10.1016/S1000-9361(11)60399-3.

Cooper, M. and Shepherd, J.E. (2008), "Single-cycle impulse from detonation tubes with nozzles", *J. Propulsion Power*, **24**(1), 81-87. https://doi.org/10.2514/1.30192.

Debnath, P. and Pandey, K.M. (2017), "Exergetic efficiency analysis of hydrogen-air detonation in pulse detonation combustor using computational fluid dynamics", *Int. J. Spray Combust. Dyn.*, **9**(1), 44-55. https://doi.org/10.1177%2F1756827716653344.

Dyer, R.S., Kaemming, T.A. and Baker, R.T. (2003), "Reaction ratio and nozzle expansion effects on the PDE performance", *Proceedings of the 39th AIAA/ASME/SAE/ASEE Joint Propulsion Conference and Exhibit*, Huntsville, Alabama, U.S.A., July.

Hsu, Y.C., Chao, Y.C. and Chung, K.M. (2018), "Detonation transmission with an abrupt change in area", *Adv. Aircraft Spacecraft Sci.*, **5**(5), 533-550. https://doi.org/10.12989/aas.2018.5.5.533.

Kailasanath, K. (2000), "Review of propulsion applications of detonation waves", *AIAA J.*, **38**(9), 1698-1708. https://doi.org/10.2514/2.1156.

Kuzmin, A. (2019), "Shock wave instability in a bent channel with subsonic/supersonic exit", *Adv. Aircraft Spacecraft Sci.*, **6**(1), 19-30. https://doi.org/10.12989/aas.2019.6.1.019

Li, Q., Fan, W., Yan, C., Hu, C. and Ye, B. (2007), "Experimental investigation on performance of pulse detonation rocket engine model", *Chin. J. Aeronaut.*, **20**(1), 9-14.

Ma, F., Choi, J.Y. and Yang, V. (2005), "Thrust chamber dynamics and propulsive performance of multitube pulse detonation engines", *J. Propulsion Power*, **21**(4), 681-691. https://doi.org/10.2514/1.8182.

Ma, F., Choi, J.Y. and Yang, V. (2005), "Thrust chamber dynamics and propulsive performance of single-tube pulse detonation engines", *J. Propulsion Power*, **21**(3), 512-526. https://doi.org/10.2514/1.7393.

Morris, C.I. (2005), "Numerical modeling of single-pulse gasdynamics and performance of pulse detonation rocket engines", *J. Propulsion Power*, **21**(3), 527-538. https://doi.org/10.2514/1.7875.

Mouronval, A.S., Hadjadj, A. Kudryavtsev, A.N. and Vandromme, D. (2002), "Numerical investigation of transient nozzle flow", *Shock Waves*, **12**, 403-411. https://doi.org/10.1007/s00193-002-0171-0.

Pandey, K.M. and Debnath, P. (2016), "Review on recent advances in pulse detonation engines", *J. Combustion*, 1-16. https://doi.org/10.1155/2016/4193034.

Shao, Y., Liu, M. and Wang, J.P. (2010), "Continuous detonation engine and effects of different types of nozzle on its propulsion performance", *Chin. J. Aeronaut.*, **23**(6), 647-652. https://doi.org/10.1016/S1000-9361(09)60266-1.

Sutton, G.P. and Oscar, B. (2010), *Rocket Propulsion Elements*, (8th Edition), John Wiley & Sons, INC.

Tangirala, V.E., Dean, A.J., Tsuboi, N. and Hayashi, A.K. (2007), "Performance of a pulse detonation Engine

under subsonic and supersonic flight conditions", *Proceedings of the 45th AIAA Aerospace Sciences Meeting and Exhibit*, Reno, Nevada, U.S.A., Janaury.

Yan, Y., Fan, W., Wang, K. and Mu, Y. (2011), "Experimental investigation of the effect of bell-shaped nozzles on the two-phase pulse detonation rocket engine performance", *Combust. Explos. Shock Waves*, **47**(3), 335-342. https://doi.org/10.1134/S0010508211030117.

Yan, Y., Fan, W., Wang, K., Zhu, X. and Mu, Y. (2011), "Experimental investigations on pulse detonation rocket engine with various injectors and nozzles", *Acta Astronautica*, **69**(1-2), 39-47. https://doi.org/10.1016/j.actaastro.2011.03.002.

CC

Abbreviations

C-J	Chapman Jouguet
CFD	Computational Fluid Dynamics
C-D	Convergent Divergent
CDE	Continuous Detonation Engine
LES	Large Eddy Simulation
Ma	Mach Number
PDE	Pulse Detonation Engine
PDRE	Pulse Detonation Rocket Engine